Carbohydrate Research 343 (2008) 2789–2796

Contents lists available at ScienceDirect

Carbohydrate Research

journal homepage: www.elsevier.com/locate/carres

Molecular structure of eight possible configurational isomers of 2,3- and 3,4-epimino derivatives of 1,6-anhydro-β-D-hexopyranoses: conformation analysis, intra- and inter-molecular hydrogen bonds

Jan Sýkora [a,*], Jindřich Karban [a], Ivana Císařová [b], Stanislav Hilgard [c]

[a] Institute of Chemical Process Fundamentals of the ASCR, v. v. i., Rozvojová 135, 165 02 Prague 6, Czech Republic
[b] Center of Molecular and Crystal Structures, Faculty of Science, Charles University, Hlavova 2030, 128 40 Prague 2, Czech Republic
[c] Department of Organic Chemistry, Faculty of Science, Charles University, Hlavova 2030, 128 40 Prague 2, Czech Republic

ARTICLE INFO

Article history:
Received 18 March 2008
Received in revised form 2 May 2008
Accepted 26 May 2008
Available online 2 June 2008

Keywords:
Epimines
Conformational analysis
X-ray crystallography
Hydrogen bonds
IR

ABSTRACT

The crystal structures of a complete series of configurational isomers of 2,3-epimino and 3,4-epimino derivatives of 1,6-anhydro-β-D-hexopyranoses were determined by single-crystal X-ray analysis. The structures exhibited conformational rigidity within the series regardless of the position and orientation of the aziridine ring. Possible formation of intramolecular hydrogen bonds involving the NH group is discussed with respect to the results of IR spectroscopy and to the intermolecular hydrogen bonds found in the crystal packing.

1. Introduction

Aziridines represent an important class of compounds since they are widely used as versatile and reactive synthetic intermediates and precursors to more complex molecules.[1–4] A few aziridine derivatives have been isolated from natural sources too[5,6] and some of them exhibited biological activities with potential in anticancer therapy.[7–13]

The most important reaction of aziridine derivatives is the cleavage of the three-membered aziridine ring. The regioselectivity of aziridine-ring cleavage of pyranose aziridines (also called epimines) depends primarily on the conformation of the pyranose ring.[14] Usually, no prediction can be made about the regioselectivity of aziridine-ring cleavage of conformationally flexible pyranose derived aziridines because the conformation in the transitional state can change readily with minimum energy. The cleavage of pyranose aziridines attains much higher degree of predictable regioselectivity in kinetically controlled reactions if the conformation of the tetrahydropyran ring is fixed by a substituent or by an additional ring.[14] Until now the stereochemistry of epimino pyranoses have been almost solely determined by NMR spectroscopy, which allows only rough estimation of the conformation in solution. Owing to the crucial role that conformation plays in the aziridine-ring cleavage, it is important to get a deeper insight into the structure of representative examples of conformationally fixed pyranose aziridines by means of X-ray crystallography that permits a detailed analysis of the compound stereochemistry. Known conformations of such derivatives determined in the solid state can represent a good starting point in conformation evaluation of these or similar compounds by other techniques. So far only one crystal structure of a pyranose derived aziridine has been published to the best of our knowledge.[15] We succeeded in crystallization of a full series of epimino derivatives of 1,6-anhydro-β-D-hexopyranoses **Ib**, **II**, **IIIb**, **IVb**, **Vb**, **VI**, **VII**, **VIIIb** (**b** denotes benzyloxy, Scheme 1) that we had prepared as a part of our research programme, and we wish to report on their crystal structure here. The synthesis and conditions of crystallization of epimines under study were reported elsewhere.[16] A brief summary of the synthesis and crystallization conditions are included in the experimental. Most of the epimines had the hydroxyl group protected as benzyl ether except for the *gulo*, *altro* and *galacto*-derivatives **II**, **VI** and **VII** in which case only free hydroxyl derivatives provided single crystals suitable for X-ray analysis. The crystal structures of all possible configurational isomers of 1,6-anhydro-2,3-dideoxy-2,3-epimino- and 1,6-anhydro-3,4-dideoxy-3,4-epimino-β-D-hexopyranoses enable us to evaluate conformational rigidity of the 6,8-dioxabicyclo-[3,2,1]-octane skeleton and/or conformational changes

* Corresponding author. Tel.: +420 220 390 307; fax: +420 220 920 661.
E-mail address: sykora@icpf.cas.cz (J. Sýkora).

0008-6215/$ - see front matter © 2008 Elsevier Ltd. All rights reserved.
doi:10.1016/j.carres.2008.05.025

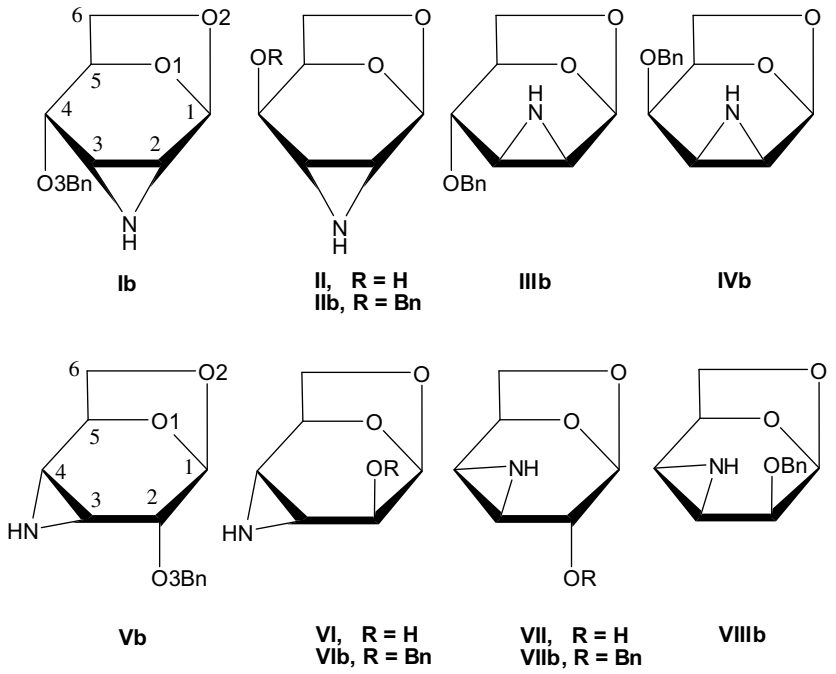

Scheme 1.

induced by configurational and positional isomerism. Furthermore, the formation of intra and intermolecular hydrogen bonds in the solid state and in solution is discussed.

2. Results and discussion

2.1. Conformational analysis

It was previously assumed that the tetrahydropyran ring of 2,3- and 3,4-epimines adopts the half-chair conformation $^{5}H_{O}$ and $^{1}H_{O}$, respectively (in the sequence of atoms C1–C2–C3–C4–C5–O1, Scheme 1).[16,17] The crystal structures of **Ib**–**VIIIb** show in fact the envelope conformation E_{O} (or E_{6} by convention used for a six-membered ring in general) of the pyranose ring in all cases. The same conformation is assumed by the already published[15] structure of 1,6-anhydro-2-*O*-benzyl-3,4-[*N*-(cyclohexyl)epimino]-3,4-dideoxy-β-D-allose which was found in CSD.[18] The E_{O} conformation found in the present study is slightly deformed (Fig. 1), because it is puckered at C5 for 2,3-epimines and at C1 for 3,4-epimines. The epimine structures thus break down into two groups almost symmetrically distributed on both sizes of the ideal E_{O} conformation (see projection in Fig. 2a). However, the deviation of C1 or C5 atom from the plane defined by C2–C3–C4–C5/C1–C2–C3–C4 atoms which indicates the transition from the envelope to a half-chair conformation is not that large, and thus the derivatives **II** and **VI** with the most significant distortion only reach the border between the envelope and half-chair conformation (for the list of ring puckering parameters[19] see Table 1 or their polar projection; Fig. 2a). It is noticeable that the structures of **II** and **VI** both represent *exo*-epimine derivatives with the hydroxyl group orientated trans with respect to the aziridine ring. In spite of these deviations from the ideal envelope conformation, the tetrahydropyran ring exhibits very restricted conformational mobility as the ring puckering parameter Φ lies in the interval of only 9.3° for the 2,3-epimines and 9.0° for the 3,4-epimines. It can be therefore expected that the pyranose ring assumes very similar conformations in solution. In such a case the regioselectivity of kinetically controlled ring opening reactions will be primarily governed by the stereochemistry of the substrate and will probably follow the Fürst-Plattner rule (preferential formation of the trans-diaxial product).

The dioxolane five-membered ring also shows two distinct ranges of conformation for the 2,3- and 3,4-epimines. The conformations of the 2,3-epimino derivatives range between a slightly deformed envelope ^{O}E (or ^{5}E by convention used for a five-mem-

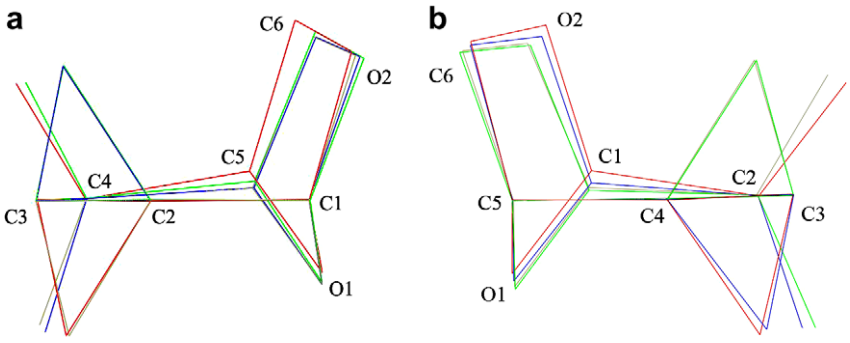

Figure 1. Comparison of the pyranose ring conformation for (a) 2,3-epimines, (b) 3,4-epimines.

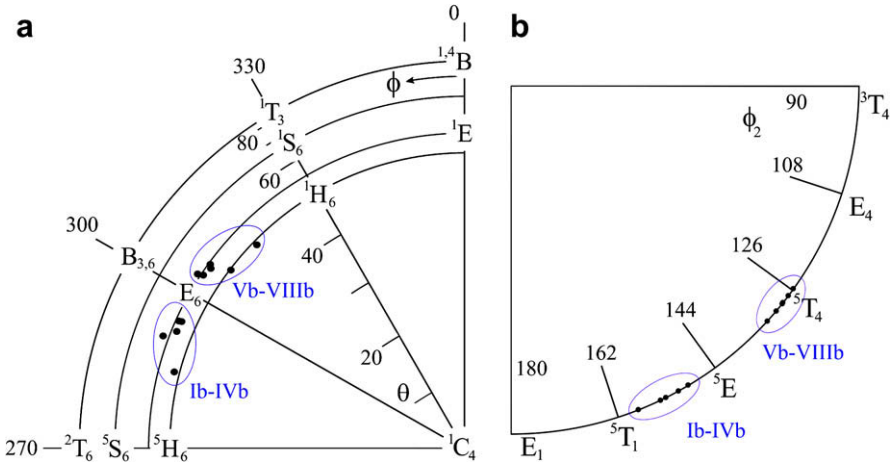

Figure 2. (a) Pyranose and (b) dioxolane ring puckering parameters projection.

Table 1
Ring puckering parameters[19] (C1–C2–C3–C4–C5–O1), (C1–O2–C6–C5–O1)

Derivative	Pyranose ring			Dioxolane ring	
	Q (Å)	θ (°)	Φ(°)	q (Å)	Φ (°)
Ib1[a]	0.625	54.6	292.4	0.416	153.5
Ib2	0.627	54.9	294.3	0.423	149.3
II	0.629	51.4	285.2	0.411	158.5
IIIb	0.631	53.7	294.5	0.433	151.2
IVb	0.65	54.2	290.8	0.435	154.5
Vb	0.615	51.7	307.6	0.420	128.5
VI	0.624	49.9	314.6	0.424	125.6
VII1	0.638	53.7	303.8	0.440	128.7
VII2	0.635	54.2	306.1	0.441	127.0
VII3	0.638	55.1	303.4	0.448	130.2
VIIIb	0.630	54.1	305.6	0.439	132.5

[a] The number of the molecule in the asymmetric unit.

bered ring in general) and twisted conformation $^{O}T_{1}$ (in the sequence of atoms C5–C6–O2–C1–O1). The 3,4-epimino derivatives range between ^{O}E and twisted conformation $^{O}T_{4}$ (see the ring puckering parameter projection; Fig. 2b), but the distribution is closer to the twisted conformation.

The X-ray structure analysis of **Ib**–**VIIIb** has revealed the expected shortening of C–C bond in the aziridine ring in both 2,3- and 3,4-aziridine derivatives when compared to the corresponding bond distance in 1,6-anhydro-β-D-hexopyranose (levoglucosan). The C–C bonds in the vicinity of the aziridine ring are apparently shortened as well (Table 2). An interesting feature found within this series is the lengthening and/or shortening of the C5–C6 bond in the 2,3- and 3,4-epimines, respectively, in comparison with the mean value of this bond for 1,6-anhydro-hexopyranoses (1.520 Å; calculated from 16 structures[18b] found in CSD). The aziridine ring forms an almost ideal equilateral triangle in the structures **Ib**–**VIIIb** (with the C–N distances ~1.47 Å and the valence angles close to 60°). The aziridine ring hydrogen atoms and the plane of the pyranose ring (C1–C2–C3–C4–C5; the oxygen atom is not involved) together form an angle in the range of 24–34° enabling an axial nucleophile attack.

2.2. Intramolecular hydrogen bonds

The crystal structure can also provide information about possible formation of intramolecular hydrogen bonds. Conclusions drawn from crystal structures about hydrogen bonding can be then compared with results obtained in solution or can complete them. The bonding possibilities of the NH group are the most interesting as the imino group is present in all compounds studied. The results of IR spectroscopy show that in solution the hydrogen bond can be accepted by all three oxygen atoms depending on the mutual spatial arrangement of the imino group and oxygen atoms (Table 3).

However, only one intramolecular hydrogen bond of the imino group was found in the solid state; in the structure of **Vb** (Fig. 3). This derivative represents the 3,4-*exo*-epimino derivative with cis-arrangement of the benzyloxy group and imino group. The hydrogen atom binds to the pyranose oxygen O1 and to a weaker degree to the oxygen of the benzyloxy group O3 with the distances NH···O 2.38 and 2.59 Å, respectively. This finding corresponds to the IR spectrum of this derivative that shows two bands indicating two bonds in the approximate intensity ratio 9:1. Similar behaviour in solution (two bands of the associated NH group) shows 2,3-*exo*-epimine **Ib** also with cis-arranged benzyloxy and imino group. No band of the free NH group was found in the IR spectra of **Ib** and **Vb**. In contrast to **Vb**, compound **Ib** does not form an intramolecular hydrogen bond in the solid state.

The imino group in the *exo*-epimines with the trans orientated benzyloxy group (**II** and **VI**) cannot create any other hydrogen bond than that to the O1, and thus the remaining less intensive bands at 3321 and 3326 cm^{-1} have to be assigned only to a free imino group.

Table 2
Bonding distances in studied epimines

	C1–C2 (Å)	C2–C3	C3–C4	C4–C5	C5–O1	O1–C1	C5–C6	C6–O2	O2–C1
2,3-Epimine[a]	1.513	1.483	1.517	1.520	1.436	1.414	1.532	1.440	1.417
3,4-Epimine[b]	1.521	1.506	1.478	1.506	1.436	1.414	1.506	1.442	1.421
Levoglucosan[c]	1.527	1.542	1.543	1.522	1.446	1.408	1.528	1.449	1.430

[a] The mean value for the 2,3-epimino derivatives.
[b] The mean value for the 3,4-epimino derivatives.
[c] The mean value for five levoglucosan structures[18a] found in CSD.

Table 3
IR data of **Ib**–**VIIIb** including benzyloxy derivatives for which suitable single crystals were not obtained (**IIb**, **VIb** and **VIIb**)

Band shape[b]	**Ib** sh	**II**[a] rd	**IIb** rd	**IIIb** rd	**IVb** ud	**Vb** sh	**VI** rd	**VIb** rd	**VII** s	**VIIb** s	**VIIIb** sh
NH (free)											
ν(NH)		3321	3323	3323	3322		3326	3327	3327	3325	3322
$\Delta\nu_{1/2}$			14	21	23		13	12	20	24	43
Rel. int. (%)			11	55	23		8	6	100	100	50
NH···OBn											
ν(NH)	3301					3302					3309
$\Delta\nu_{1/2}$	14					16.5					14
Rel. int. (%)	12					13					50
NH···O2											
ν(NH)				3304	3309						
$\Delta\nu_{1/2}$				18	15						
Rel. int. (%)				45	77						
NH···O1											
ν(NH)	3285	3293	3289			3288	3295	3294			
$\Delta\nu_{1/2}$	15		14			16	14	16			
Rel. int. (%)	88		89			87	92	94			

[a] Compound is almost insoluble in CCl_4, it is not possible to obtain the data with the demanded accuracy; band at 3321 is weaker.
[b] s—singlet, rd—resolved doublet, sh—shoulder, ud—unresolved doublet with an asymmetry at higher wavenumbers; ν(NH)—the wavenumbers of the stretching vibrations of the NH group (cm^{-1}); $\Delta\nu_{1/2}$—the half-widths of the bands (cm^{-1}); rel. intensities are given in per cents of the integrated absorption intensity related to the sum of intensities of all bands.

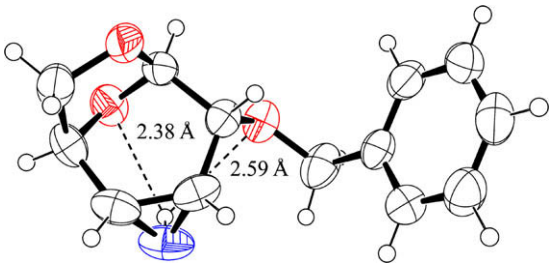

Figure 3. Intramolecular hydrogen bonds in **Vb**; ORTEP projection.

The *endo*-epimine derivatives (**IIIb**, **IVb** and **VII**, **VIIIb**) could stabilize their molecule with a hydrogen bond to the 1,6-anhydro oxygen O2. However, the crystal structures reveal a steric hindrance of C6–H_{endo} hydrogen which prevents the imino hydrogen from reaching the O2 lone pair (Fig. 4). The IR spectra of both **IIIb** and **IVb** (2,3-epimines), on the other hand, contain two similar bands in the NH region. One band was attributed to the NH···O2 bond and the second to the free NH group as no other explanation is meaningful for the trans-derivative **IIIb**. These results indicate that the $H6_{endo}$ hindrance is more effective towards the O3 atom. A slight conformation distortion in solution is also conceivable

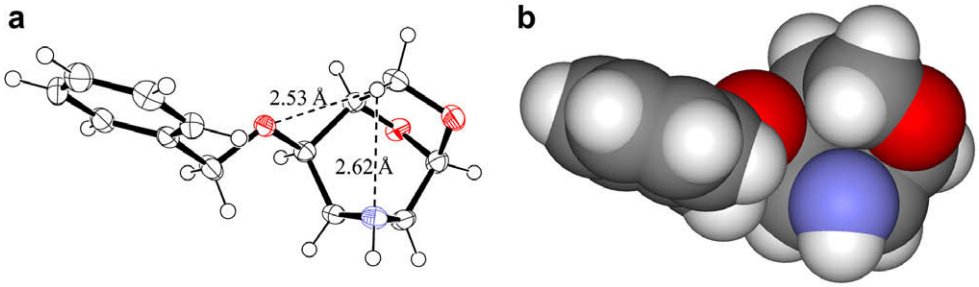

Figure 4. (a) ORTEP projection of steric hindrance of $H6_{endo}$ atom in **IVb** and (b) space filling presentation of crystal structure **IVb**.

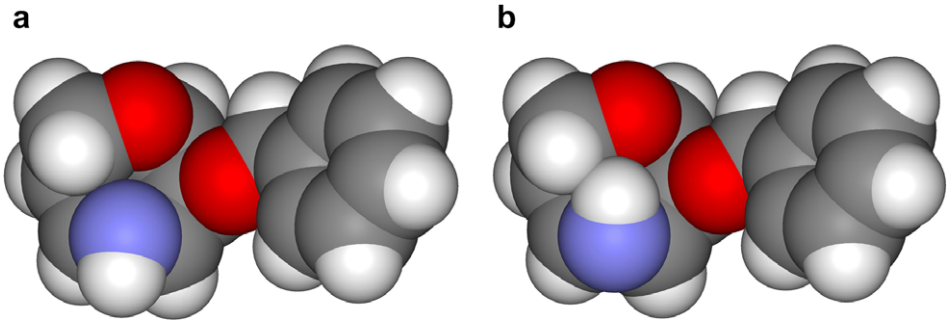

Figure 5. Space filling presentation of crystal structure (a) **VIIIb** and (b) **VIIIb** with the inverted stereochemistry on the nitrogen atom showing the hindrance of $H6_{endo}$ atom.

for the purpose of additional molecule stabilization via an intramolecular hydrogen bond to O2.

Table 4
Intermolecular interaction in the crystal structures **Ib**–**VIIIb**

Intermolecular bond	Distance (Å)
Ib	
N–H(1)···N(2)	2.29
N–H(1)···O1(2)	2.68
N–H(1)···O3(2)	2.84
N–H(2)···N(1)	2.28
N–H(2)···O1(1)	2.84
C6–H_{endo}(2)···O3(1)	2.82
II	
O3–H···O4	1.93
O4–H···N	1.95
N–H···O3	2.35
O4–H···O1	2.67
C6–H_{exo}···O2	2.67
C3–H···O1	2.78
N–H···O1	2.87
IIIb	
N–H···O2	2.24
N–H···N	2.93
C6–H_{exo}···O3	2.78
C5–H···Bn	2.94[a]
C11–H···Bn	3.00[a]
IVb	
N–H···Bn	2.54[a]
C2–H···O3	2.46
C1–H···O1	2.60
C12–H···Bn	2.89[a]
Vb	
N–H···O1	2.53
C4–H···O1	2.80
C6–H_{exo}···O1	2.79
C7–H···O2	2.72
C12–H···Bn	3.02[a]
C9–H···Bn	3.01[a]
VI	
N–H···O3	2.28
O3–H···N	2.01
C4–H···O1	2.59
C6–H_{endo}···O1	2.60
C3–H···O2	2.61
C2–H···O2	2.67
C5–H···O2	2.83
VII	
N–H(1)···N(3)	2.25
O3–H(1)···N(1)	1.96
C5–H(2)···O1(1)	2.80
C6–H_{endo}(1)···O1(1)	2.62
C6–H_{exo}(2)···O3(1)	2.87
C6–H_{exo}(1)···O3(1)	2.87
N–H(2)···O3(3)	2.18
C4–H(2)···O2(2)	2.54
O3–H(2)···N(2)	2.06
O3–H(3)···O3(2)	1.90
C3–H(3)···O3(2)	2.72
N–H(3)···O2(3)	2.38
C4–H(1)···O2(3)	2.49
N–H(2)···O3(3)	2.18
C1–H(2)···O3(3)	2.60
VIIIb	
N–H···O3	2.41
N–H···N	2.66
N–H···O2	2.41
C12–H···O1	2.62
C11–H···O1	2.66
C4–H···O2	2.76
C12–H···O2	2.75
C6–H_{endo}···Bn	2.89[a]

[a] Interaction with the π-system of the benzyloxy group.

The $H6_{endo}$ hindrance should be even bigger in **VII** and **VIIIb** (3,4-epimines) because the NH group is closer to the $H6_{endo}$ atom (Fig. 5), and indeed a band of an associated imino group does not appear in the IR spectrum of **VII** and **VIIb**. The band at 3309 cm^{-1} in the spectrum of compound **VIIIb** was ascribed to the NH···O3 bond because the NH···O2 bond is unlikely owing to its absence in the spectrum of epimines **VII** and **VIIb**.

2.3. Intermolecular hydrogen bonds

Only one of the studied epimines forms an intramolecular hydrogen bond in the solid state. It is compound **Vb**, as it was discussed above in 2.2. All other epimines form only intermolecular hydrogen bonds in the solid state. The nitrogen lone pair of these epimines plays the role of the hydrogen bond acceptor, and it is turned into the middle of the carbohydrate moiety. The hydrogen bond donor in the structures containing the benzyloxy group is the NH group from a neighbouring molecule (**Ib**, **IIIb**, **IVb**, **VIIIb**) as the hydrogen atom points out of the sugar moiety and joins the intermolecular hydrogen bond network. The hydrogen bond donor in the structures containing the free hydroxyl is either the hydroxyl group (**VI**, **VII**) or a water molecule (**II**) (for the list of intermolecular interactions see Table 4).

All epimines with a cis-arrangement of the three-membered ring and the benzyloxy group form a triangle-shaped 'cavity' (Fig. 6a) between O2–N1–O3 for the *endo*-(**IVb**, **VIIIb**) and between O1–N1–O3 for the *exo*-epimines (**Ib**, **Vb**). This space is convenient for the acceptance of a hydrogen atom of another molecule as demonstrates crystal structure **Ib** (Fig. 6b). In the case of the crystal structure **IVb**, the cavity is already partially occupied by $H6_{endo}$ (with the distances C6-H_{endo}···O3 2.53 and C6–H_{endo}···N 2.62 Å) as mentioned above and cannot play the role of a hydrogen bond acceptor. The imino group therefore prefers interaction with the phenyl ring of an adjacent molecule. The distance NH··· the plane of the phenyl ring is 2.54 Å and indicates strong interaction between the hydrogen and the π-system of the aromatic ring. Since the structure **Vb** uses the 'cavity' space for intramolecular interaction, other interactions prevail in molecular packing. Oxygen atoms accept weak hydrogen bonds from the hydrogen atoms at C4, C6 and C7 carbon atoms and CH–π interaction between benzyloxy groups appears. The steric hindrance of $H6_{endo}$ in structure **VIIIb** results in the absence of an intramolecular hydrogen bond to O2, but it is negligible for the accessibility of the O2–N1–O3 cavity by the NH group from another molecule (compare with Fig. 5a). Similarly to **Ib**, the imino hydrogen is attracted to the space between O2–N1–O3 atoms in this structure. The hindrance of $H6_{endo}$ appears again in the molecular packing of **IIIb** (the distances C6–H_{endo}···N 2.72 Å) indicating possible general behaviour of 2,3-*endo*-epimines (together with the already discussed packing of **IVb**). The NH group binds significantly only to O2 of a neighbouring molecule. Furthermore, CH–π interactions take place in the molecular packing of **IIIb**.

The crystallizations of the benzyloxy derivatives of the epimines **IIb**, **VIb** and **VIIIb** were unsuccessful, only single crystals of the free hydroxyl derivatives **II**, **VI** and **VII** were prepared. This difference in hydroxyl group protection has probably only negligible influence on the pyranose ring conformation discussed above in Section 2.1, but the presence of a free hydroxyl group can significantly influence the intermolecular hydrogen bonding network and consequently the molecular packing in these structures. It is the hydrogen atom of the hydroxyl group in **VI** and **VII** (or of water molecule in **II**) which binds to the nitrogen lone pair. These hydrogen bonds are well orientated towards the nitrogen lone pair and are much stronger than hydrogen bonds in molecular packing of the benzyloxy derivatives.

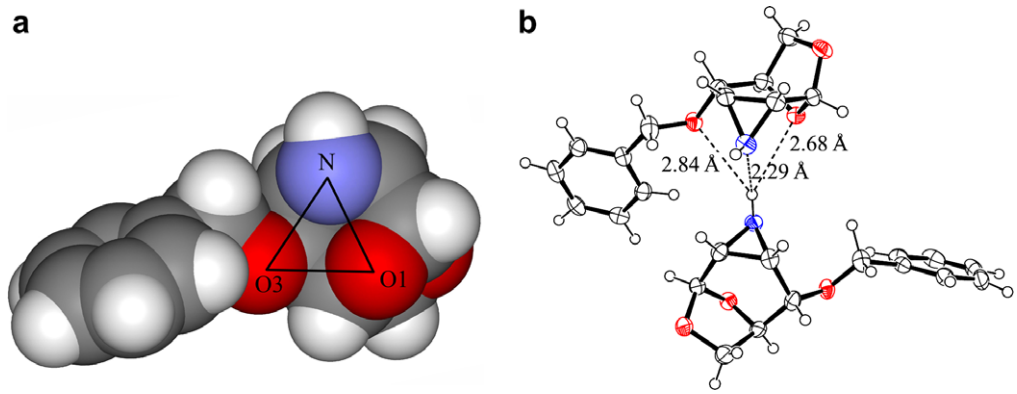

Figure 6. (a) Space filling presentation of crystal structure **Ib** showing the triangle cavity and (b) ORTEP projection of intermolecular interaction in **Ib**.

3. Conclusion

The compounds **Ib**–**VIIIb** represent a complete series of configurational isomers of epimino derivatives of 1,6-anhydro-β-D-hexopyranoses and also the largest set of epimino carbohydrates for which the crystal structures are now available. The assumption that the tetrahydropyran ring adopts the half-chair conformations $^{5}H_{O}$ or $^{1}H_{O}$ was proved incorrect. The ring adopts a distorted envelope conformation E_{O} in all cases, and there is no significant difference between the *exo*- and *endo*-aziridine derivates within the 2,3- or 3,4-epimines. Conformational changes induced by configurational changes are insignificant and testify to great rigidity of the pyranose ring. Accordingly, we expect that the aziridine-ring opening reactions in solution will proceed under stereochemical control.

Infrared spectroscopy at low concentrations in the region of stretching vibrations of the imino group enables us to distinguish three different types of the imino group association on the basis of known configuration. The assignment of the bands thus can indirectly confirm the structure of measured compounds.

Some general rules/features have been found in the molecular packing of the structures **Ib**–**VIIIb** that might be useful for the prediction of molecular packing/association of similar molecules.

4. Experimental

4.1. Synthesis

Epimino derivatives **Ib**, **IIIb**, **IVb**, **Vb**, **VIb**, **VIIb** and **VIIIb** were obtained by reductive cyclization of suitable vicinal *trans*-azido tosylates with lithium aluminium hydride in tetrahydrofuran. Epimino derivatives **II** and **VI** were prepared by the aza-Payne rearrangement of suitable vicinal amino epoxides obtained *in situ* from vicinal azido epoxides by lithium aluminium hydride reduction in tetrahydrofuran. Introduction of the azide functionality into the carbohydrate molecule was achieved by nucleophilic cleavage of 1,6:2,3- and 1,6:3,4-dianhydroderivatives of β-D-hexopyranoses with NaN_3 in $MeOCH_2CH_2OH/H_2O$. Syntheses of epimines **Ib** and **II** in Scheme 2 illustrate the synthetic protocol. Compounds **IIb** and **VIb** were prepared by O-benzylation of **II** and **VI** with BnBr/NaH.

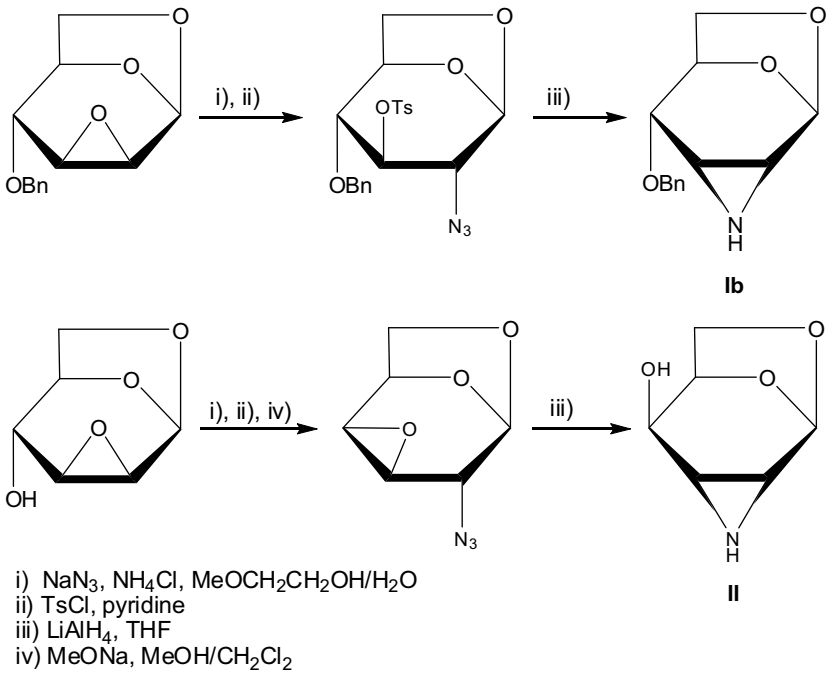

Scheme 2.

Compound **VII** was prepared by debenzylation of **VIIb**. For full details of the synthesis and NMR spectra of compounds **Ib**–**VIIIb** see Ref. 16.

4.2. IR spectroscopy

The IR spectra were measured on a Perkin–Elmer 684 spectrometer in tetrachloromethane solution at concentration below 4.2×10^{-3} mol/L to prevent intermolecular association. 60–120 scans were collected in order to obtain a satisfactory signal-to-noise ratio at a nominal resolution of 2.5 cm^{-1}. Parameters of the overlapping bands were obtained by computer band separation assuming Cauchy profile of bands; minimal accuracy is 1 cm^{-1} for ν_{max} and 2 cm^{-1} for $\Delta\nu_{1/2}$.

4.3. Crystallographic data

Suitable single crystals of compounds **Ib**, **IVb** and **VIIIb** were crystallized from diethyl ether, compounds **II** and **VI** from methanol–diethyl ether, compound **IIIb** was crystallized from acetone–diethyl ether, compound **Vb** from diethyl ether–petroleum ether and compound **VII** from ethanol–diethyl ether.

Diffraction data were collected using CAD4-MACHIII diffractometer (Enraf-Nonius) with the graphite monochromated Mo Kα radiation. Cryostream Cooler (Oxford Cryosystem) was used for the low temperature measurements. The structures were solved by direct methods and refined by full-matrix least-squares on F^2 values (SIR92,[20] SHELXL97[21]). All heavy atoms were refined anisotropically. Hydrogen atoms were localized from the expected geometry and only their positions were refined. The imino and hydroxyl hydrogen atoms were localized from difference electron density map and were refined isotropically. PARST97[22] was used for the ring puckering parameters calculation and ORTEP-3[23] (ellipsoid probability 50%) and Accelrys DS Visualizer[24] for structure presentation.

The crystallographic data for the structures reported in this paper have been deposited with the Cambridge Crystallographic Data Centre as supplementary publication. Copies of the data can be obtained free of charge on application to CCDC, e-mail: deposit@ccdc.cam.ac.uk.

4.3.1. X-ray of Ib

$2C_{13}H_{15}NO_3$, M = 466.52 g/mol, monoclinic system, space group $P2_1$, a = 5.688(4), b = 18.284(9), c = 10.980(9) Å, β = 90.21(6)°, Z = 2, V = 1141.9(1) Å^3, D_c = 1.36 g cm^{-3}, μ(Mo Kα) = 0.10 mm^{-1}, T = 150 K, crystal dimensions of 0.4 × 0.4 × 0.25 mm. The independent part is created by two sugar molecules. The structure converged to the final R = 0.0293 and R_w = 0.0774 using 2069 independent reflections for 427 parameters (θ_{max} = 24.98°). CCDC registration number 679063.

4.3.2. X-ray of II

$C_6H_9NO_3 \cdot 1/2H_2O$, M = 152.15 g/mol, monoclinic system, space group $C2$, a = 11.633(2), b = 5.991(1), c = 9.890(1) Å, β = 100.29(1)°, Z = 4, V = 678.2(1) Å^3, D_c = 1.49 g cm^{-3}, μ(Mo Kα) = 0.12 mm^{-1}, T = 293 K, crystal dimensions of 0.4 × 0.3 × 0.2 mm. The independent part is created by one sugar moiety and half of the water molecule. The structure converged to the final R = 0.0334 and R_w = 0.0873 using 654 independent reflections for 136 parameters (θ_{max} = 24.95°). CCDC registration number 679064.

4.3.3. X-ray of IIIb

$C_{13}H_{15}NO_3$, M = 233.26 g/mol, monoclinic system, space group $P2_1$, a = 5.7079(3), b = 6.4972(7), c = 16.2769(8) Å, β = 99.960(4)°, Z = 2, V = 594.54(4) Å^3, D_c = 1.30 g cm^{-3}, μ(Mo Kα) = 0.09 mm^{-1}, T = 293 K, crystal dimensions of 0.7 × 0.3 × 0.1 mm. The structure converged to the final R = 0.0258 and R_w = 0.0683 using 1150 independent reflections for 215 parameters (θ_{max} = 24.97°). CCDC registration number 679065.

4.3.4. X-ray of IVb

$C_{13}H_{15}NO_3$, M = 233.26 g/mol, orthorhombic system, space group $P2_12_12_1$, a = 6.5418(9), b = 10.180(1), c = 17.262(3) Å, Z = 4, V = 1149.6(3) Å^3, D_c = 1.35 g cm^{-3}, μ(Mo Kα) = 0.10 mm^{-1}, T = 150 K, crystal dimensions of 0.5 × 0.5 × 0.2 mm. The structure converged to the final R = 0.0300 and R_w = 0.0750 using 1467 independent reflections for 214 parameters (θ_{max} = 26.96°). CCDC registration number 679066.

4.3.5. X-ray of Vb

$C_{13}H_{15}NO_3$, M = 233.26 g/mol, monoclinic system, space group $P2_1$, a = 5.8910(6), b = 7.775(3), c = 12.718(1) Å, β = 96.399(8)°, Z = 2, V = 578.9(2) Å^3, D_c = 1.34 g cm^{-3}, μ(Mo Kα) = 0.10 mm^{-1}, T = 293 K, crystal dimensions of 0.6 × 0.6 × 0.2 mm. The structure converged to the final R = 0.0271 and R_w = 0.0742 using 1226 independent reflections for 215 parameters (θ_{max} = 25.96°). CCDC registration number 679067.

4.3.6. X-ray of VI

$C_6H_9NO_3$, M = 143.14 g/mol, monoclinic system, space group $P2_1$, a = 5.3078(5), b = 8.1433(5), c = 7.3907(7) Å, β = 99.125(8)°, Z = 2, V = 315.41(5) Å^3, D_c = 1.51 g cm^{-3}, μ(Mo Kα) = 0.12 mm^{-1}, T = 293 K, crystal dimensions of 0.5 × 0.5 × 0.2 mm. The structure converged to the final R = 0.0271 and R_w = 0.0762 using 981 independent reflections for 128 parameters (θ_{max} = 29.94°). CCDC registration number 679068.

4.3.7. X-ray of VII

$3C_6H_9NO_3$, M = 429.42 g/mol, monoclinic system, space group $P2_1$, a = 6.2086(9), b = 10.324(2), c = 14.586(2) Å, β = 94.190(5)°, Z = 2, V = 932.4(3) Å^3, D_c = 1.53 g cm^{-3}, μ(Mo Kα) = 0.12 mm^{-1}, T = 293 K, crystal dimensions of 0.4 × 0.4 × 0.1 mm. The independent part is created by three sugar molecules. The structure converged to the final R = 0.0273 and R_w = 0.0644 using 1741 independent reflections for 380 parameters (θ_{max} = 24.97°). CCDC registration number 679069.

4.3.8. X-ray of VIIIb

$C_{13}H_{15}NO_3$, M = 233.26 g/mol, orthorhombic system, space group $P2_12_12_1$, a = 6.3584(4), b = 9.8444(7), c = 18.4781(8) Å, Z = 4, V = 1156.6(1) Å^3, D_c = 1.34 g cm^{-3}, μ(Mo Kα) = 0.10 mm^{-1}, T = 293 K, crystal dimensions of 0.4 × 0.4 × 0.15 mm. The benzyloxy groups is disordered into two positions. It was necessary to apply some geometrical restrains to the phenyl moiety. Hydrogen atoms were placed there from the expected geometry and were not refined. This model converged to the final R = 0.0420 and R_w = 0.1021 using 2266 independent reflections for 166 parameters (θ_{max} = 25.96°). CCDC registration number 679070.

Acknowledgements

This work was supported by the Grant Agency of the Academy of Sciences of the CR (Grant Nos. IAA400720703 and IAA400720706) and by the Ministry of Education of the Czech Republic (Grant No. MSM0021620857).

Supplementary data

Supplementary data associated with this article can be found, in the online version, at doi:10.1016/j.carres.2008.05.025.

References

1. Tanner, D. *Angew. Chem., Int. Ed. Engl.* **1994**, *33*, 599–619.
2. Osborn, H. M. I.; Sweeney, J. *Tetrahedron: Asymmetry* **1997**, *8*, 1693–1715.
3. Sweeney, J. B. *Chem. Soc. Rev.* **2002**, *31*, 247–258.
4. Zwanenburg, B.; ten Holte, P. In *Stereoselective Heterocyclic Synthesis Iii*, **2001**; Vol. 216, pp 93–124.
5. Naganawa, H.; Usui, N.; Takita, T.; Hamada, M.; Umezawa, H. *J. Antibiot.* **1975**, *28*, 828–829.
6. Legters, J.; Thijs, L.; Zwanenburg, B. *Tetrahedron* **1991**, *47*, 5287–5294.
7. Kasai, M.; Kono, M. *Synlett* **1992**, 778–790.
8. Tomasz, M.; Mercado, C. M.; Olson, J.; Chatterjee, N. *Biochemistry* **1974**, *13*, 4878–4887.
9. Fukuyama, T.; Xu, L. H.; Goto, S. *J. Am. Chem. Soc.* **1992**, *114*, 383–385.
10. Armstrong, R. W.; Moran, E. J. *J. Am. Chem. Soc.* **1992**, *114*, 371–372.
11. Yokoi, K.; Nagaoka, K.; Nakashima, T. *Chem. Pharm. Bull.* **1986**, *34*, 4554–4561.
12. Jones, R. J.; Rapoport, H. *J. Org. Chem.* **1990**, *55*, 1144–1146.
13. Coleman, R. S.; Carpenter, A. J. *J. Org. Chem.* **1992**, *57*, 5813–5815.
14. Karban, J.; Kroutil, J. *Adv. Carbohydr. Chem. Biochem.* **2006**, *60*, 28–104.
15. McAuliffe, J. C.; Skelton, B. W.; Stick, R. V.; White, A. H. *Aust. J. Chem.* **1997**, *50*, 209–218.
16. Karban, J.; Buděšínský, M.; Černý, M.; Trnka, T. *Collect. Czech. Chem. Commun.* **2001**, *66*, 799–819.
17. Černý, M.; Elbert, T.; Pacák, J. *Collect. Czech. Chem. Commun.* **1974**, *39*, 1752–1767.
18. (a) Cambridge Structure Database, CSD version 5.29, January 2008 release (a) CSD codes of 5 used levoglucosan structures, AHGLPY01, AHGLPY10-13.; (b) CSD codes of 16 used 1,6-anhydro-hexopyranoses structures, ACHGAL, AHGALP, AHGLPY01, AHGLPY10-13, ANALPR, AWOMAA, AWOMOO, AWONIJ, BIFTUF, HUDDUF, LEVGTA, QIJCIV, QIJMEB.
19. Cremer, D.; Pople, J. A. *J. Am. Chem. Soc.* **1975**, *97*, 1354–1358.
20. Altomare, A.; Burla, M. C.; Camalli, M.; Cascarano, G.; Giacovazzo; Guagliardi, A.; Polidori, G. *J. Appl. Crystallogr.* **1994**, *27*, 435.
21. Sheldrick, G. M. SHELXL97. Program for Crystal Structure Refinement from Diffraction Data; University of Göttingen: Göttingen, 1997.
22. Nardelli, M. *J. Appl. Crystallogr.* **1995**, *28*, 659.
23. Farrugia, L. J. *J. Appl. Crystallogr.* **1997**, *30*, 565.
24. Accelrys Software Inc., Accelrys DS Visualizer version 1.7, 2008. www.accelrys.com.